



ELSEVIER

Physica C 378–381 (2002) 1185–1190

PHYSICA C

www.elsevier.com/locate/physc

# Study of the relation between evaluation of strain distribution on superconducting coil and mechanical heat generation

Hiroshi Seino <sup>a,\*</sup>, Minoru Kurihara <sup>a</sup>, Toshiki Herai <sup>a</sup>, Eiji Suzuki <sup>b</sup>

<sup>a</sup> *Railway Technical Research Institute, 2-8-38, Hikari-cho, Kokubunji-shi, Tokyo 185-8540, Japan*

<sup>b</sup> *Central Japan Railway Company, 1-6-6, Yaesu, Chuou-ku, Tokyo 103-0028, Japan*

Received 27 September 2001; accepted 25 January 2002

## Abstract

In the superconducting Maglev system, on-board superconducting magnets (SCMs) are vibrated at various frequencies according to the train speed by the electromagnetic disturbance which is caused when the train passes over ground coils. Then a mechanical loss is generated inside the inner vessel in the SCM. This phenomenon increases the heat load on the cryogenic equipment in the SCM. It has been surmised that the mechanical heat inside the inner vessel is generated by the frictional heat caused by the relative microscopic slips between fasteners and superconducting coil (SC coil). Nevertheless, heat generation mechanisms inside the inner vessel have not been studied sufficiently. In this study, we suggest a hypothesis that the frictional heat generated by the relative microscopic slips between fasteners and a SC coil will be indicated if the calculated strain distribution on the SC coil is evaluated. The results of this study supported this hypothesis.

© 2002 Elsevier Science B.V. All rights reserved.

PACS: 75; 81.40.R

Keywords: Superconducting devices; Magnet; Vibration; Maglev; Heat

## 1. Introduction

In the superconducting Maglev system, the mechanical loss inside the inner vessel in the on-board superconducting magnets (SCMs) has been evaluated by the vibration test results of the superconducting coil (SC coil) under a purely me-

chanical lateral force by using a hydraulic servo actuator [1,2]. The eigenvibration modes of the SC coil which involve coil deformation such as bending or twisting were strongly related to the increases in the mechanical heat generation in the lateral vibration [3,4].

However, in a recent study, the mechanical heat generation phenomena caused by vibration were confirmed without remarkable SC coil deformation under vertical SCM vibration.

Therefore, the mechanical loss inside the inner vessel is studied from the viewpoint of relative

\* Corresponding author. Tel.: +81-425-73-7301; fax: +81-425-73-7300.

E-mail address: [seino@rtri.or.jp](mailto:seino@rtri.or.jp) (H. Seino).

microscopic slips between the fasteners and SC coil inside the inner vessel.

Vertical force added mechanical vibration tests for the SC coil installed into inner vessel was adopted to evaluate the mechanical heat generation inside the inner vessel for the reason of model simplification.

## 2. Structure of the SCM and SC coil [1,2]

A cryostat of SCM mainly consists of SC coils, inner and outer vessels, refrigerant tanks and radiation shield. The SC coil is installed in the inner vessel with intermediate coil fasteners which are arranged on the race-track shaped SC coil at equal intervals. A radiation shield is installed in the space between inner and outer vessels. SC coils are primarily cooled by liquid helium in the inner vessel, and secondarily cooled by liquid nitrogen at a radiation shield. These two cooling stages are insulated by vacuum and a support structure. The inner vessel is rigidly supported in the outer vessel by using heat insulated support columns. Three types of support columns are used between inner and outer vessels to correspond to the three-dimensional force of electrodynamic suspension, in the way that the longitudinal, lateral and vertical supports correspond to the propulsion, guidance and levitation force, respectively.

## 3. Experimental

Fig. 1 shows a schematic of the vertical SC coil vibration test system.

The SC coil installed into inner vessel was fastened to the dummy outer vessel by 10 support columns without longitudinal ones. Then, the SC coil and the dummy outer vessel were cooled within a vacuum chamber with liquid helium and liquid nitrogen, respectively. A vibration force was applied to the dummy outer vessel through separation bellows by a hydraulic servo actuator that was set on the vacuum chamber.

The SC coil installed into inner vessel was vibrated under magnetized and non-magnetized

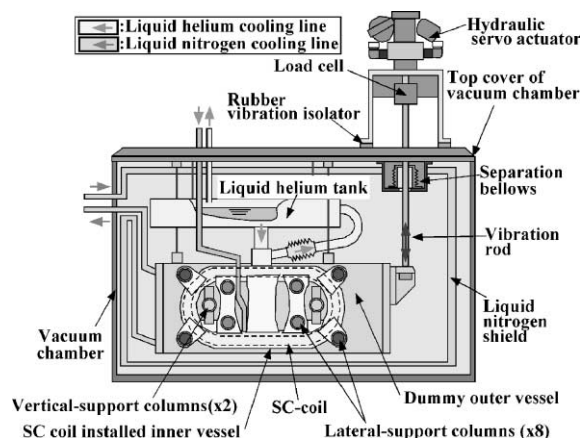


Fig. 1. Schematic of the vertical SC coil vibration test system.

states, with whole support columns fixed and outward lateral-support columns removed.

Helium evaporation from the inner vessel was measured by using a helium flowmeter. The mechanical loss caused by vibration was indicated by the increase in the volume of evaporation helium gas when the SC coil was vibrated. The vibration of the SC coil installed into inner vessel and the dummy outer vessel were measured by accelerometers. The temperature change of the inner vessel surface was measured by CGR temperature sensors. The temperature data were calibrated by a heating test of the inner vessel surface.

## 4. Experimental results

The SC coil deformation has been evaluated by the inner vessel deformation, under the assumption that these two categories of deformation are identical (SC coil = inner vessel).

There was no difference in the vibration dependence of the increase in the helium evaporation (= helium loss) between magnetized and non-magnetized states. Therefore, the helium loss during vertical SC coil vibration was a mechanical loss.

It can be surmised that helium loss during vibration was not a hysteresis loss of the support column, by reason that the temperature of the inner vessel surface which surrounded support columns did not change during vibration. Accordingly, it can be assumed that the helium loss

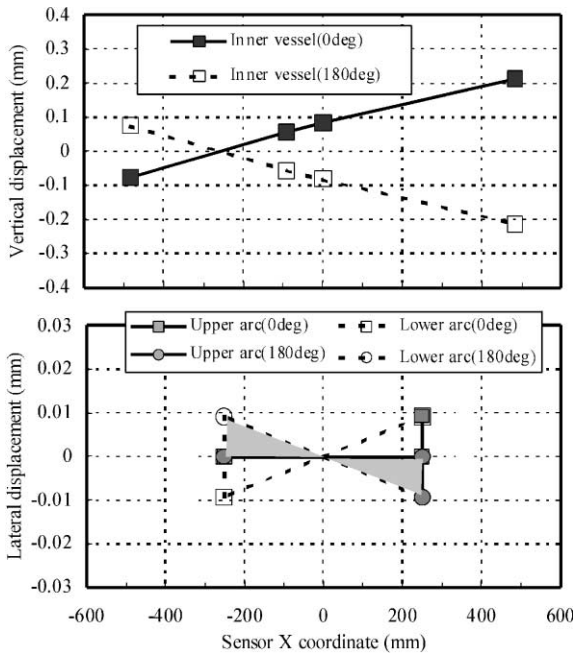


Fig. 2. An example of SC coil vibration mode under a vertical vibration.

during vibration was generated inside the inner vessel presumably due to frictional heating.

Fig. 2 shows the typical SC coil vibration mode under vertical vibration. In this figure, vibration mode is shown by the vertical or lateral vibration displacements which are calculated from accelerometer output by double integration for different

points on the SC coil.  $X = 0$  indicates the longitudinal center of the SC coil.

Translating and pitching vibration modes in vertical movement were confirmed. A small twisting vibration mode was confirmed at the lower arc of SC coil in lateral movement.

Fig. 3 shows the comparison of helium loss sensitivity and the SC coil twisting deformation between lateral and vertical vibration test results. A deformation coefficient of the twisting SC coil is expressed by averaged twisting velocity (ATV). The ATV was evaluated by summing up the amplitudes at the typical spots on the circumference of the SC coil, which express the eigentwisting vibration mode [4]. The calculation aids of the ATV are also shown in Fig. 3.

SC coil twisting under vertical vibration is smaller than that under lateral vibration. However, the helium loss sensitivity to the SC coil twisting deformation under vertical vibration is larger than that under lateral vibration. This result demonstrates that the helium loss under vertical vibration was caused except for that caused by SC coil twisting deformation.

The relationship between the vertical SC coil vibration and the helium loss was evaluated from the standpoint of SC coil vertical load which was input from support columns. The coefficient of weighted frequency total load (FTL) of SC coil was used for evaluation. FTL was defined by using the equation shown in Fig. 4.

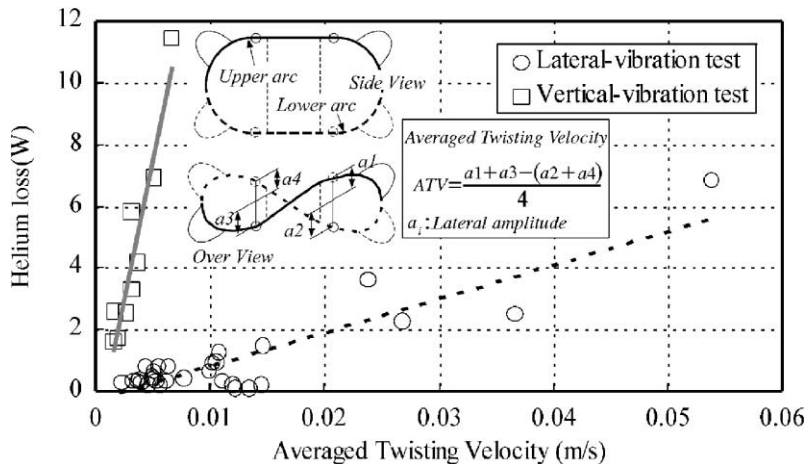


Fig. 3. Comparison of helium loss sensitivity to the SC coil twisting between lateral and vertical vibration test results.

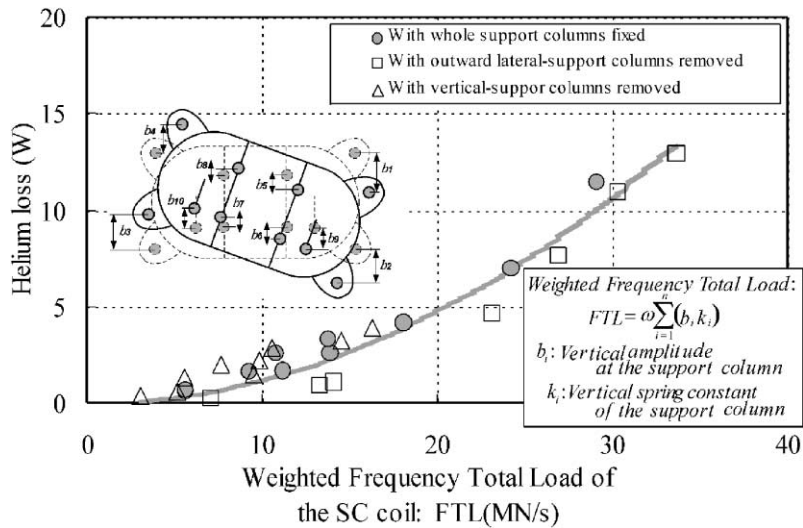


Fig. 4. Helium loss versus weighted FTL.

Fig. 4 shows the coefficient of FTL dependence of the helium loss for various inner vessel supporting conditions in vertical SC coil vibration tests. There was a close correlation between helium loss and FTL. The helium loss increased proportionally to the square of FTL. This result suggests that the helium loss (= mechanical loss) was generated by the transmitted load from support columns into the SC coil.

##### 5. Consideration of the mechanical heat generation inside the inner vessel

The heat generation inside the inner vessel was analyzed from the standpoint of frictional heat by the finite element method (FEM). It can be assumed that the frictional phenomena inside the inner vessel occurred at contact surfaces between the inner vessel and coil fasteners, or between SC coil and coil fasteners. The inner vessel and the coil fastener are in metal–metal contact. The SC coil and the coil fastener are in metal and polymer contact with epoxy or polyimide (Kapton tape). Both contacts are connected in series at the load path from the support column to the SC coil. The frictional coefficient in fretting at the temperature of 4 K can be assumed to be 0.3 in metal–polymers, sticking in metal–metal contact [5]. Therefore, the

frictional heat inside the inner vessel occurs at the contact surface between coil fasteners and SC coil, due to the foregoing frictional coefficient data.

Static structural analysis of FEM added with vertical acceleration was performed to evaluate the heat generation area inside the inner vessel. The FEM analysis model consisted of an inner vessel, coil fasteners and SC coil under rigid connection. The support columns of the SC coil were substituted with three-dimensional spring elements which input the measured stiffness. The heat generation area inside the inner vessel was evaluated based on the assumption that the calculated strain at the surface of the SC coil shows the frequency of microscopic slips between the coil fasteners and SC coil. The examples of SC coil strain distribution obtained by FEM analysis were shown in Fig. 5.

The abscissa and coordinate axes indicate the position of the coil fastener and corresponding equivalent strain of SC coil, respectively. The coil fastener nos. 3–8 correspond to the positions of outward flanges which are attached to the lateral-support columns to prevent SC coil twisting. The coil fasteners 5–8 which are at the lower arc of the SC coil correspond to the position of vertical-support column joint. The strain data corresponding to the positions of outward flanges (coil fasteners 3–8) were larger than those on the other part. The strain at the coil fastener 6 of the lower

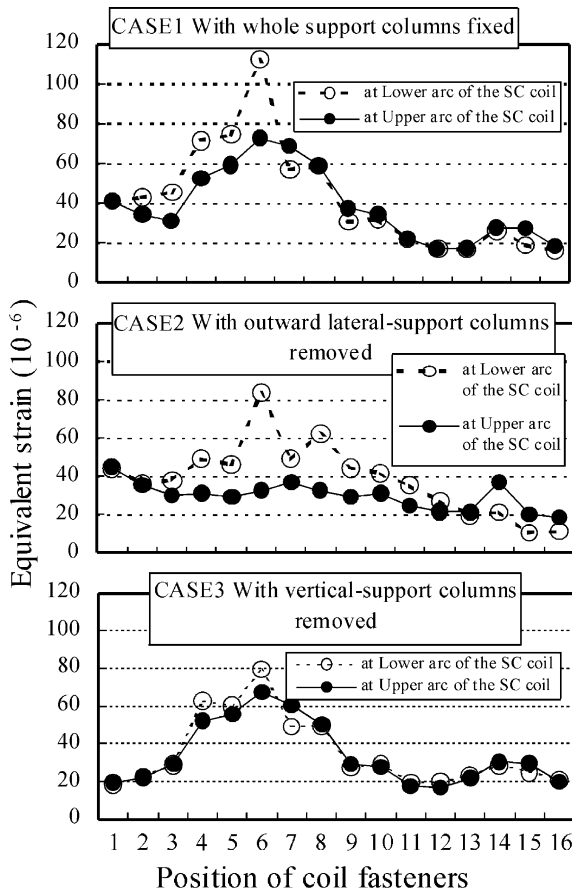


Fig. 5. Strain distributions of SC coil (FEM analysis results).

arc also jitted out when compared with that at the upper arc. SC coil strains corresponding to the position of the outward flange at the upper arc and the vertical-support joint are almost nil when lateral-support columns of outward flange are removed, and when vertical-support columns are removed. Based on the result of the SC coil strain distribution analysis, it was surmised that frictional heat was generated at the contact between coil fasteners and SC coil near support columns.

### 6. Verification of the SC coil strain distribution analysis

The validity of the SC coil strain distribution analysis to estimate the heat generation area was

examined. For the purpose of reducing the heat generation, it was considered in SC coil strain distribution analysis to reduce the SC coil strain at SC coil lower arc which was affected by the vertical-support columns. An additional plate reinforced inner vessel was also prepared based on the result of analysis, and the effect to reduce heat generation was examined by using a vertical SC coil vibration test system. The strain reducing effect at the SC coil lower arc obtained by SC coil strain distribution analysis is shown in Fig. 6. A comparison of the vertical SC coil vibration test results between standard and additional plate reinforced inner vessels is shown in Fig. 7. In both cases, the SC coil installed into inner vessel was vibrated without outward lateral-support columns,

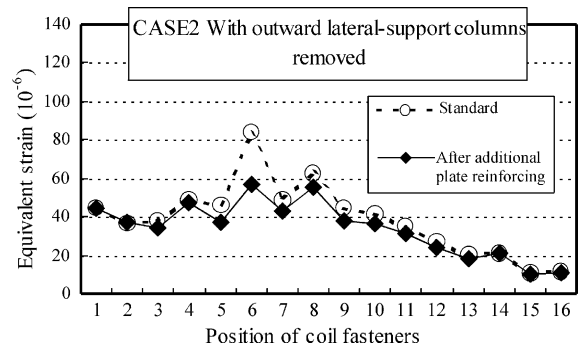


Fig. 6. A comparison of SC coil strain distributions between standard and additional plate reinforcing inner vessels.

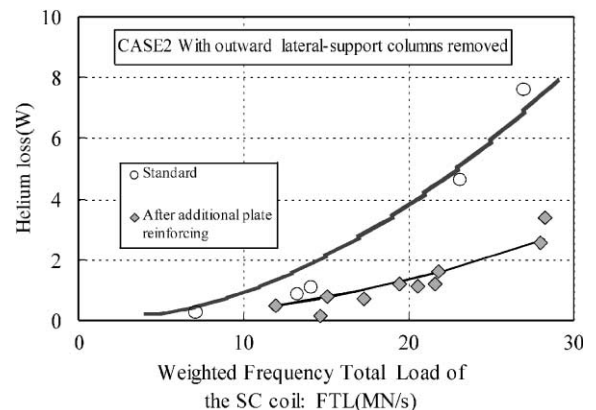


Fig. 7. A comparison of vertical SC coil vibration test results between standard and additional plate reinforcing inner vessels.

to clarify the frictional loss reducing effect. The frictional loss of the additional plate reinforcing inner vessel during vibration was reduced to 40% of that of the standard inner vessel. The validity of the SC coil strain distribution analysis to reduce the frictional loss inside the inner vessel was suggested from this result.

## 7. Conclusions

The relation between SC coil vibration and helium loss (or mechanical loss) was examined by using a vertical SC coil vibration test system. The vibration test result suggested that the mechanical loss inside the inner vessel was generated by the transmitted load from the support columns into the SC coil.

SC coil strain distribution analysis by the static structural FEM was performed to consider the frictional heat inside the inner vessel. The heat generation area inside the inner vessel was evaluated based on the assumption that the calculated strain at the surface of the SC coil shows the frequency of microscopic slips between the coil fasteners and SC coil. The analysis result suggests that frictional heat occurs in the surrounding area of the support columns. The validity of the SC coil strain distribution analysis to estimate the heat generation area was examined by comparing the analysis and vertical SC coil vibration test results between the standard and heat-reducing inner

vessels. The results of examination prove the validity of the SC coil strain distribution analysis.

The results of this study demonstrate that the SC coil strain distribution analysis is an effective method to reduce the mechanical heat generation inside the inner vessel.

## Acknowledgements

This study is financially supported by the Ministry of Land, Infrastructure and Transport, Japan.

## References

- [1] M. Terai, S. Inadama, H. Tsuchishima, E. Suzuki, T. Okai, Development of new superconducting magnets for the Yamanashi Test, in: Proc. of Maglev '95, Bremen, Germany, October, 1995, pp. 267–273.
- [2] E. Suzuki, M. Terai, T. Takizawa, M. Yamaji, Y. Jizo, Superconducting magnet for Maglev Train, in: Proc. Int. Conf. Speedup Technology for Railway and Maglev Vehicles, Yokohama, Japan, November, 1993, pp. 352–357.
- [3] S. Nakagaki, T. Syudo, M. Yamaji, S. Matsuda, T. Uchida, M. Terai, A. Miura, Vibration analysis of superconducting magnets for Maglev, in: Proc. Int. Conf. Speedup Technology for Railway and Maglev Vehicles, Yokohama, Japan, November, 1993, pp. 358–363.
- [4] T. Yamaguchi, Y. Jizo, H. Akagi, M. Terai, M. Igarashi, M. Shinobu, Vibration characteristics and mechanical heat load of superconducting magnet of Maglev, in: Proc. Maglev '98, Yamanashi, Japan, April, 1998, pp. 244–249.
- [5] A. Iwabuchi, T. Honda, J. Tani, Tribological properties at temperatures of 293, 77 and 4 K in Fretting, *Cryogenics* 29 (1989) 124–131.